ELASTIC SCATTERING OF DEUTERONS BY TRITONS

O.O. BELYUSKINA, V.I. GRANTSEV, V.V. DAVYDOVSKYY, K.K. KISURIN, S.E. OMELCHUK, G.P. PALKIN, YU.S. ROZNYUK, B.A. RUDENKO, L.S. SALTYKOV, V.S. SEMENOV, L.I. SLUSARENKO, B.G. STRUZHKO, V.K. TARTAKOVSKY, V.A. SHYTIUK

Institute for Nuclear Research, Nat. Acad. of Sci. of Ukraine
(47, Nauky Ave., Kyiv 03680, Ukraine; e-mail: interdep@kinr.kiev.ua)

UDC 539.172.17

Differential cross-sections of elastic scattering of deuterons with the energy $E_d = 37.0$ MeV by tritons have been measured in the range of scattering angles $25^\circ \leq \theta_{\text{c.m.}} \leq 150^\circ$. The angular distributions at elastic scattering of deuterons by tritons (helions) at energies of 14–40 MeV have been analyzed in the framework of a microscopic diffraction nuclear model and taking NN interactions into account. This allowed the angular distributions of deuterons near the main maximum ($\theta_{\text{c.m.}} \leq 60^\circ$) at $E_d = 14.4$, 37.0, and 39.9 MeV to be described satisfactorily. An explanation for the origin of a broad secondary maximum that appears at low energies of incident deuterons is proposed. The corresponding calculations have been carried out to prove that it appears due to the interference between quantum and classical amplitudes of isotropic scattering and as a manifestation of the structure of colliding nuclei. The characteristic features that emerge in the angular dependence of the *dt* scattering cross-sections in the interval $60^\circ \leq \theta_{\text{c.m.}} \leq 130^\circ$, when the energy increases from 6 to 40 MeV, has been explained only qualitatively, using the phenomenological quasiclassical approximation. The energy spectra of deuterons and recoil tritons in the T(dd)T reaction at $E_d = 37.0$ MeV have been analyzed.

1. Introduction

The nuclear physics of few-nucleon systems is, to some extent, a special branch of nuclear physics. It has the own specificity. The processes of collisions between deuterons and tritons at energies of tens and hundreds kiloelectronvolts, when the overcoming of the nuclear Coulomb barrier becomes possible – as well as other processes with light nuclei – are intensively studied in connection with the researches of nuclear reactions that are running in the Sun and other stars, and also in connection with the project of controlled thermonuclear synthesis. The Coulomb interaction between very light nuclei still plays an important role at indicated low collision energies.

However, the *dt* collisions at much higher energies of tens megaelectronvolts remain insufficiently studied [1–7], despite that they are rather informative and interesting from the viewpoint of studying the structure of few-nucleon nuclei and the nuclear interaction. The Coulomb interaction at the energies of deuterons bombarding tritons in the interval 6–40 MeV makes a very small contribution (of the order of 1%) to the scattering cross-section, which is also associated with minimal possible nuclear charges of hydrogen isotopes ^{2}H and ^{3}H, a collision between which is considered. Therefore, in what follows, we neglect the Coulomb interaction, when calculating the cross-sections of *dt* scattering. For the same reason, the d^3He scattering is quite similar to the *dt* one [7].

At the deuteron energies concerned, the wavelength (divided by 2π) $\lambda\!\!\!^{-}$ of the relative motion of ^{2}H and ^{3}H nuclei turns out several times smaller than the radius of their nuclear interaction $R_N \approx 4 \div 6$ fm. Therefore, when calculating the elastic scattering cross-sections of deuterons by tritons, the diffraction approximation can be used. It means that the consideration will actually be quasiclassical ($\lambda\!\!\!^{-} \ll R_N$). In this case, the influence of a number of quantum-mechanical effects (the Pauli principle, nuclear spins, wave function antisymmetrization) becomes appreciably weaker [8], which allows the calculations to be made considerably simpler. As will be shown below, it is possible to perform the microscopic description of the *dt* scattering process, by using the NN interaction. In our case of dt collisions, we approximately solve the problem of interaction among five nucleons from the continuous energy spectrum within the diffraction nuclear model.

This work aims at reporting the results of our experiments on the elastic scattering of 37.0-MeV deuterons by tritons. We also present the relevant theoretical consideration and description, making use of simple quasiclassical methods. The literature data on *dt* and d^3He scattering in the energy range $E_d = 14 \div 40$ MeV were also used in our analysis.

2. Experimental Part

Elastic scattering of deuterons by tritium nuclei at the energy $E_d = 37.0$ MeV was experimentally studied on

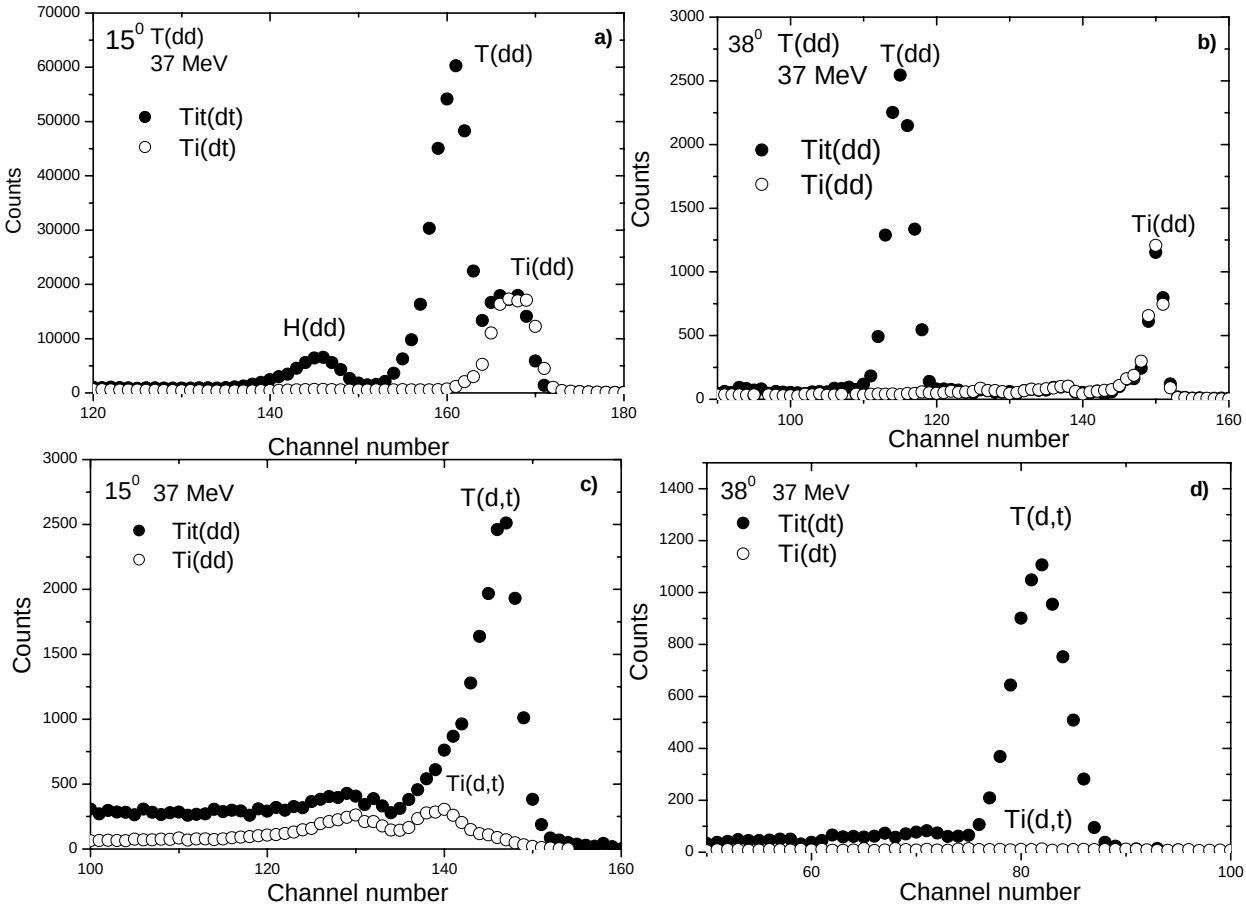

Fig. 1. (*a* and *b*) Deuteron spectra obtained with Ti–T and Ti targets at angles of 15 and 38° and at an initial energy of deuterons of 37 MeV. (*c* and *d*) The same dependences for recoil tritons

an U-240 isochronous cyclotron at the Kyiv Institute for Nuclear Research (KINR) of the National Academy of Sciences of Ukraine. A deuteron beam from the accelerator was transported to a scattering chamber in the experimental box. A strict collimation of the transported beam was provided by slot-hole diaphragms and quadrupole lenses. The measurements were carried out making use of a titanium–tritium (Ti–T) and a pure titanium target. The former target was fabricated at the KINR following a new technology. It was a Ti film 4.9 mg/cm^2 in thickness, saturated by tritium to an activity of 7.57 Cu. The equivalent thickness of tritium in the titanium matrix was 0.30 ± 0.04 mg/cm^2. Charged particles were registered making use of three telescopes (ΔE–E) located in the reaction plane. The statistical error of inclusive spectrum measurements was 1–3%, depending on the registration angle. The intensity of the ionic beam passed through the target was registered with the help of a Faraday cup connected to a current integrator. The absolute values of cross-sections were determined with an accuracy of about 15%. The energy calibration of spectra was carried out making use of the elastic and inelastic deuteron scatterings on a carbon target.

To obtain the angular distributions for the elastic dt scattering in a wide angular range, the differential cross-sections of recoil tritons were used together with the differential cross-sections of elastic deuteron scattering. Deuterons were registered in the angular interval $15° \leq \theta_{\text{l.s.}} \leq 58°$ and tritons in the interval $15° \leq \theta_{\text{l.s.}} \leq 52°$. The experimental technique and our previous results were reported in works [1, 6, 9].

2.1. Spectra

In Figs. 1,*a* and *b*, the deuteron spectra measured for Ti–T and Ti targets at angles of 15 and 38°, respectively, are depicted. Figures 1,*c* and *d* demonstrate the same

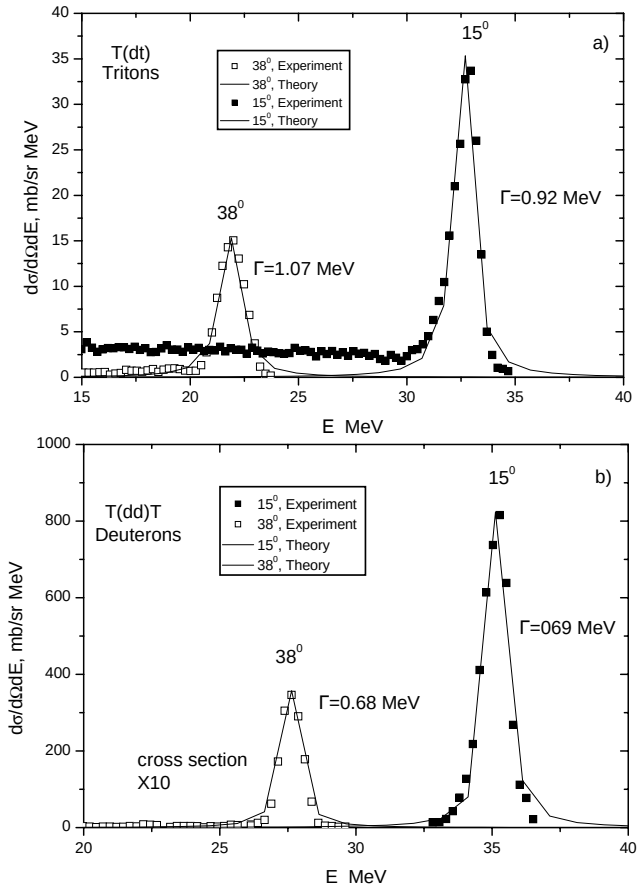

Fig. 2. (*a*) Energy spectra of deuterons elastically scattered by tritium nuclei at angles of 15 and 38° and at the initial energy of deuterons $E_d = 37$ MeV. (*b*) The same dependences for recoil tritons. Solid and dash-dotted curves display the results of calculations in the framework of the microscopic diffraction nuclear model (Eqs. (3) and (6)–(8) [20])

spectra measured at the same scattering angles but for recoil tritons. Owing to a high tritium saturation of the Ti film, the yields of deuterons and tritons from the tritium layer was several times higher than those from the Ti matrix. The resolution of a peak that corresponds to the elastic scattering of deuterons by tritons, including small angles ($\theta_{\text{l.s.}} \approx 15°$), and a peak of the deuteron elastic scattering on titanium (as well as on hydrogen) was not complicated. The peaks associated with the elastic scattering of deuterons by tritons were obtained by subtracting the spectra measured on Ti targets from those obtained for Ti–T ones, provided the same target thicknesses and equal charges in the Faraday cup. A similar procedure was carried out to resolve peaks that correspond to recoil tritons. The energy calibration of spectra was done taking advantages

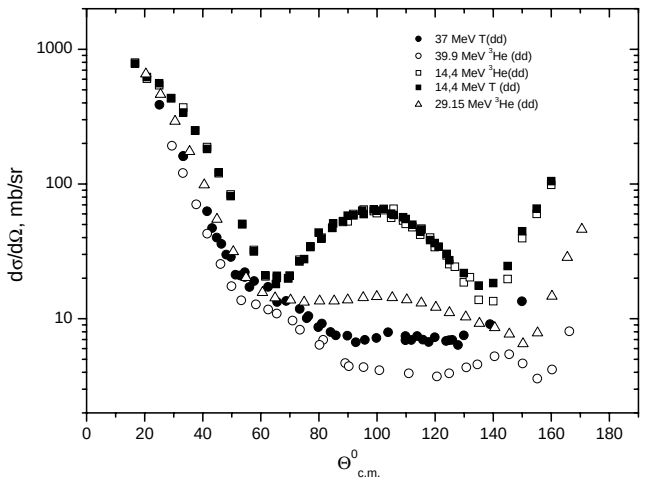

Fig. 3. Angular distributions of the deuteron scattering by tritons at deuteron energies of 14.4 [7] and 37 MeV (our data) and by helions at energies of 14.4 [7], 29.15 [10], and 39.9 MeV [11]. The energy are specified in the laboratory system

of data on the elastic and inelastic deuteron scatterings on a carbon target. The energy spectra for deuterons and recoil tritons in the T(dd)T reaction obtained at angles of 15 and 38° are illustrated in Fig. 2. The corresponding analysis is made in Section 4.4.

2.2. Angular distributions

The angular distributions $\frac{d\sigma}{d\Omega}$ of the deuteron scattering by tritons were obtained in the scattering angle range $15° \leq \theta_{\text{l.s.}} \leq 58°$ by analyzing the spectra of the elastic deuteron scattering by tritium nuclei, and in the range $46.6° \leq \theta_{\text{l.s.}} \leq 111.4°$ by analyzing the spectra of recoil tritons. The dependences of the differential cross-section $\frac{d\sigma}{d\Omega}$ on the scattering angle in the center-of-mass system (c.m.s.), taking recoil tritons into account, are exhibited in Fig. 3.

The elastic scattering of deuterons by tritons was experimentally studied only at low energies of 6.6 – 14.4 MeV [7]. Therefore, we make a comparison with the literature data on ^{3}He(dd) scattering obtained at higher energies [10, 11]. In Fig. 3, the data on the elastic *dt* scattering at energies of 14.4 [7] and 37 MeV (our results) and on the ^{3}He(d,d) scattering at 14.4 [7], 29.15 [10], and 39.9 MeV [11] are depicted. The energy values are indicated in the laboratory system (l.s.). All angular distributions are illustrated with a statistical error only.

The angular distributions are characterized by a drastic reduction of the cross-section when the scattering

angle increases to $\theta_{\rm c.m.} \leq 60^\circ$, which is characteristic of the scattering processes of weakly bound particles in few-nucleon systems. In the angular range $60^\circ \leq \theta_{\rm c.m} \leq 130^\circ$ and at $E_d = 37$ and 39.9 MeV, the cross-sections change monotonously and grow a little only at angles $\theta_{\rm c.m} \geq 130^\circ$. If the initial energy of deuterons increases, the character of the angular dependences of the elastic dt and d^3He scattering cross-sections change considerably in the range of scattering angles $60^\circ \leq \theta_{\rm c.m} \leq 130^\circ$. A broad maximum, which was observed at $\theta_{\rm c.m} \approx 100^\circ$ at an energy of 14.4 MeV, disappears at 37.0 MeV. The disappearance of the maximum at the angle $\theta_{\rm c.m} \approx 100^\circ$ is also testified by the data on d^3He scattering obtained at an energy of 29.15 MeV [10] (Fig. 3). For an energy of 39.9 MeV [11], the elastic scattering by helions has an almost the same angular dependence, as the elastic scattering of deuterons by tritons does at our energy.

3. Formalism

To consider the deuteron scattering by tritons theoretically, we use the diffraction formalism of works [8, 12–15].

3.1. Microscopic diffraction model

Let us proceed from the interaction between each of three nucleons of a ^{3}H nucleus, on the one hand, and each of two nucleons of a ^{2}H nucleus, on the other hand. To describe nuclear collisions in the c.m.s., we use nucleon-nucleon profile functions of the Gaussian type [8, 15],

$$\omega_{ij} \equiv \omega(\left|\boldsymbol{\rho}_{ij}\right|) = a\exp(-b^2\rho_{ij}^2), \tag{1}$$

where $\boldsymbol{\rho}_{ij}$ is the component of the vector $\mathbf{r}_{ij} = \mathbf{r}_i - \mathbf{r}_j$ perpendicular to the momentum $\mathbf{k}_d$ of the incident deuteron in the laboratory reference frame, $\mathbf{r}_i$ is the radius-vector of the i-th triton's nucleon ($i = 1, 2, 3$), and $\mathbf{r}_j$ the radius-vector of the j-th deuteron's nucleon ($j = 4, 5$).

Function (1) phenomenologically describes NN interactions. The values for the parameters a and b in expression (1) for energies concerned were taken approximately equal to those in works [8, 15]. Taking the correction of the parameters into account – which is needed, because the parameters depend on the energy E_d – their values were confined to the intervals

$$0.5 \leq a \leq 0.8; \quad 0.32\,\mathrm{fm}^{-1} \leq b \leq 0.55\,\mathrm{fm}^{-1}. \tag{2}$$

The profile functions ω_{ij} are related to the scattering matrices Ω_{ij} by a simple formula $\omega_{ij} = 1 - \Omega_{ij}$.

The amplitude of the elastic deuteron scattering by tritons in the diffraction approximation can be presented in the general form as a multiple integral

$$A(\boldsymbol{\chi}) = \int d^{(3)}\boldsymbol{\rho}_1 \int d^{(3)}\mathbf{r} \int d^{(3)}\mathbf{s} \int d^{(2)}\mathbf{R}_\perp\, \varphi_d^2(\mathbf{s}) \times$$

$$\times \varphi_t^2\left(\boldsymbol{\rho}_1, \mathbf{r}\right) \psi_{\boldsymbol{\chi}}^*\left(\mathbf{R}_\perp\right) \psi_0\left(\mathbf{R}_\perp\right) \times$$

$$\times \left(\Omega_{14}\Omega_{15}\Omega_{24}\Omega_{25}\Omega_{34}\Omega_{35} - 1\right), \tag{3}$$

The corresponding differential elastic-scattering cross-section which determines the angular distribution of deuterons scattered into a solid angle $d\Omega$ looks like ($\hbar = c = 1$)

$$d\sigma = \frac{k^2}{(2\pi)^2}\left|A(\boldsymbol{\chi})\right|^2 d\Omega, \quad k = \frac{3}{5}k_d, \tag{4}$$

where k is the relative momentum. The internal wave functions of a deuteron, $\varphi_d(\mathbf{s})$, and a triton, $\varphi_t(\boldsymbol{\rho}_1, \mathbf{r})$, that enter into formula (3) depend on the relative vectors (the Jacobi variables)

$$\mathbf{s} = \mathbf{r}_{45} = \mathbf{r}_4 - \mathbf{r}_5,\ \boldsymbol{\rho}_1 = \mathbf{r}_1 - \frac{\mathbf{r}_2 + \mathbf{r}_3}{2},\ \mathbf{r} = \mathbf{r}_2 - \mathbf{r}_3. \tag{5}$$

Let the coordinate origin be at the deuteron center of masses ($\mathbf{r}_5 = -\mathbf{r}_4$). Then, the vector that connects the centers of masses of a deuteron and a triton coincides with the radius-vector of the triton center of masses $\mathbf{R} = \frac{1}{3}(\mathbf{r}_1 + \mathbf{r}_2 + \mathbf{r}_3)$. The double integration over $\mathbf{R}_\perp$ in (3) is carried out over the plane perpendicular to the relative momentum $\mathbf{k} = \frac{3}{5}\mathbf{k}_d$. At the same time, the relative motion of a deuteron and a triton before and after the scattering is described by the wave functions $\psi_0(\mathbf{R}_\perp)$ and $\psi_{\boldsymbol{\chi}}(\mathbf{R}_\perp)$, respectively, in the same plane [12]. Those functions have the following simple forms:

$$\psi_0(\mathbf{R}_\perp) = 1, \quad \psi_{\boldsymbol{\chi}}(\mathbf{R}_\perp) = e^{i\boldsymbol{\chi}\mathbf{R}_\perp}. \tag{6}$$

Here, $\boldsymbol{\chi}$ is the component of the scattered deuteron momentum, which is perpendicular to the vector $\mathbf{k}$ in the diffraction approximation, its magnitude is approximately equal to $\chi = 2k\sin\theta/2$, and $\theta \equiv \theta_{\rm c.m.}$ is the angle of the deuteron scattering in the c.m.s. In the diffraction approximation and under our conditions, the angle θ does not exceed an angle of about 65° in the diffraction approximation (in the laboratory reference frame, this angle is at most 40°).

At arbitrary internal wave functions in integral (3), the amplitude $A(\boldsymbol{\chi})$ contains rather a large number

of integrals. To fulfil the integration in formula (3) explicitly, we used simple wave functions of the Gaussian type for a deuteron, $\varphi_d(\mathbf{s})$, and a triton $\varphi_t(\boldsymbol{\rho}_1, \mathbf{r})$ [8]:

$$\varphi_d(\mathbf{s}) = \left(\frac{2\lambda^2}{\pi}\right)^{3/4} e^{-\lambda^2 s^2}, \quad \lambda = 0,267\,\mathrm{fm}^{-1}, \tag{7}$$

$$\varphi_t(\rho_1, \mathbf{r}) = \frac{3^{3/4}\alpha^3}{\pi^{3/2}} e^{-\alpha^2(\rho_1^2 + \frac{3}{4}r^2)}, \quad \alpha = 0.375\,\mathrm{fm}^{-1}. \tag{8}$$

Taking into account that, at the energy of incident deuterons $E_d = \frac{k_d^2}{4M} = 37.0$ MeV, this case is considered by us most often—the main contribution to the scattering is given by relatively small angles $\theta \leq 60^\circ$, we confine the consideration to the cross-section in the momentum approximation, when the expression in parentheses in formula (3), i.e. the product of Ω_{ij} multipliers, can be approximately substituted by a simpler expression, which contains a sum of ω_{ij} terms, namely, by $-(\omega_{14} + \omega_{15} + \omega_{24} + \omega_{25} + \omega_{34} + \omega_{35})$. Then, using Eqs. (1) and (6)–(8), we obtain the following simple, compact, and explicit expression for the angular distribution of deuterons, which describes the scattering well, but only at angles $\theta_{\mathrm{c.m.}} \leq 60^\circ$:

$$\frac{d\sigma}{d\Omega} = \frac{9a^2k^2}{b^4} \exp\left[-\chi^2\left(\frac{1}{2b^2} + \frac{1}{9\alpha^2} + \frac{1}{16\lambda^2}\right)\right],$$

$$\chi = 2k\sin\frac{\theta}{2}, \quad k = \frac{1}{\lambda} = \frac{6}{5}\sqrt{ME_d}, \tag{9}$$

where M is the nucleon mass.

3.2. Quasiclassical approximation at $U_0 \to \infty$

In order to analyze the angular distributions of scattered deuterons at angles $\theta_{\mathrm{c.m.}} > 60^\circ$, i.e. the cross-sections obtained by us in the angular interval $60^\circ \leq \theta_{\mathrm{c.m.}} \leq 150^\circ$, where the absolute value of the cross-section is very small, we have to go beyond the diffraction approximation which is valid only for small scattering angles. It can be done approximately, by taking advantage of quasiclassical (because, in our case, $\lambda\!\!\!^{-} \ll R_N$) expressions for the scattering amplitude and the scattering cross-section obtained earlier [16] for two impermeable balls (i.e. when the potential energy of their interaction U_0 is infinitely large at distances shorter than R_N) which imitate a deuteron and a triton without regard for their nucleon structure. At $kR_N \gg 1$, the quasiclassical amplitude of scattering for such impermeable balls reads [16]

$$f(\theta) = i\frac{R_N}{2\sin\frac{\theta}{2}} J_1\left(2kR_N\sin\frac{\theta}{2}\right) -$$

$$-\frac{i}{2}R_N \exp\left(-2ikR_N\sin\frac{\theta}{2}\right) \tag{10}$$

at every angle $\theta_{\mathrm{c.m.}} \leq 180^\circ$. In this formula, the first term on its right-hand side looks like the known diffraction (quantum-wave) amplitude, which gives the main contribution to the cross-section at small scattering angles (the Fraunhofer diffraction). The second term is referred to as the amplitude of the classical isotropic scattering, and it provides the main contribution at large $\theta_{\mathrm{c.m.}}$, where the cross-section $\frac{d\sigma}{d\Omega} = |f(\theta)|^2$ tends to the constant value $\frac{1}{4}R_N^2$. The interference between those two amplitudes in the cross-section $\frac{d\sigma}{d\Omega} = |f(\theta)|^2$ at $\lambda\!\!\!^{-} \ll R_N$ should be small, according to the results of work [16]. Note that, in our case, the value of R_N is such that the product $kR_N \approx 5$ at the energies concerned, so that actually the condition $kR_N \gg 1$ is at the limit of its validity range. Therefore, if scattering amplitude (10) is used, the interference between the diffraction and classical amplitudes in the cross-section [16], which is usually neglected, can affect the cross-section behavior in our case. Such a situation is really observed in our calculations, as will be demonstrated below. In addition, the deuteron and the triton are not absolutely impermeable, which can result in some reduction of the cross-section. This fact can be taken into consideration at a qualitative level, if we introduce an energy-dependent parameter of semitransparency a_0 into the general profile functions ($a_0 < 1$; for a black nucleus, $a_0 = 1$) [17, 18].

For the potential energy of interaction between colliding nuclei that are considered as balls and with a finite potential well depth U_0, an explicit expression for the scattering cross-section can be also found in the Born approximation [19], when, under our conditions, $U_0 \ll \frac{1}{R_N}\sqrt{\frac{E_d}{M}} \approx 10$ MeV. However, this approximation cannot be used explicitly even for a qualitative estimation.

The problem considered in work [16] can be made even more complicated by introducing the potential energy of interaction between nuclei, U_0, that has a finite value at internuclear distances shorter than R_N. However, the cross-section cannot be obtained in the explicit form in this case. Below, we consider some other crude approximations which qualitatively explain the

cross-section behavior at large scattering angles θ. In particular, it is the classical limit $\lambda \to 0$, when an explicit expression for the scattering cross-section can be written down in the case of a finite potential well depth U_0.

4. Analysis of Experimental Results

When analyzing experimental results, we used the differential cross-sections of the elastic dt scattering $\frac{d\sigma}{d\Omega}$ (in units of mb/sr) in the c.m.s., which we obtained at a deuteron energy of 37.0 MeV, as well as the corresponding literature data for an energy of 14.4 MeV [7] and the data on the d^3He scattering at an energy of 39.9 MeV [11]. When comparing the results of theoretical calculations with experimental data, we present our data making allowance for both the statistical error and the error associated with the absolutization of cross-sections.

4.1. Microscopic diffraction and impermeable nucleus models

In Figs. 4 to 6, the results of calculations of the cross-section angular dependences obtained in the framework of various theoretical approaches and at various energies are depicted. The calculations that use formula (9) of the microscopic diffraction model in the momentum approximation, which is valid only at small angles $\theta_{\text{c.m.}} \leq 60°$, bring about curves *1* in Fig. 4 at the following parameters: $a = 0.5$, $b = 0.32$ fm^{-1} ($E_d = 14.4$ MeV); $a = 0.8$, $b = 0.55$ fm^{-1} ($E_d = 37$ MeV); and $a = 0.7$, $b = 0.55$ fm^{-1} ($E_d = 39.9$ MeV). The results of calculations by formula (10), which is valid at every angle, at $R_N = 5.2$ fm for $E_d = 14.4$ MeV and at $R_N = 4.4$ fm for $E_d = 14.4$ and 39.9 MeV are exposed in Fig. 4 by curves *2*. Amplitude (10) also includes the parameter $a_0 = 0.7 \div 1.0$, which is analogous to the parameter a in expression (1). As was expected, formula (9) describes the observed cross-sections rather well in its angular range $\theta_{\text{c.m.}} \leq 60°$ (solid curves *1* in Fig. 4), because they were obtained in the framework of the microscopic consideration of collisions between deuterons and tritons with regard for NN interactions [20].

Formula (10) gives almost the same description (Figs. 4,*b* and *c*) of the cross-section behavior at small angles $\theta_{\text{c.m.}} \leq 60°$, as formula (9) does, despite that it was obtained in the framework of a phenomenological consideration of nuclear scattering, when nuclei were considered as impermeable continuous balls. Since the

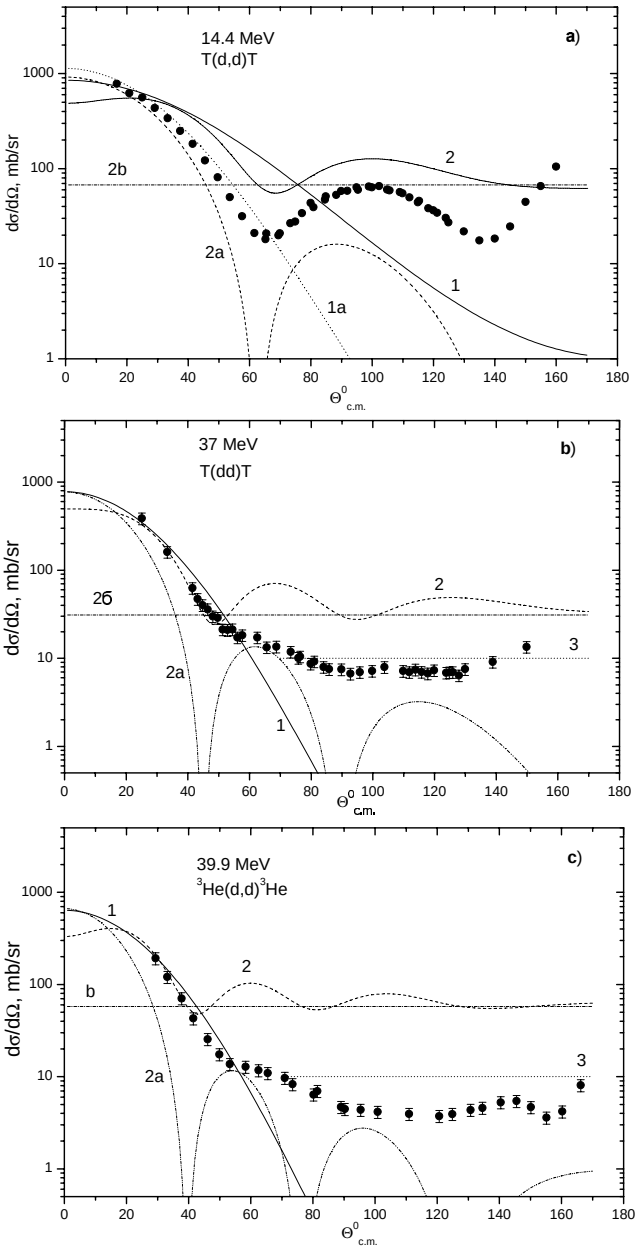

Fig. 4. Comparison between theoretical and experimental angular distributions at energies of 14.4 (a), 37 (b), and 39.9 MeV (c). Curves *1* are the result of calculations in the framework of the microscopic diffraction nuclear model (9) with the following parameters: (a) $a = 0.50$, $b = 0.32$ fm^{-1}; (b) $a = 0.80$, $b = 0.55$ fm^{-1}; and (c) $a = 0.70$, $b = 0.55$ fm^{-1}. Curves *2* are the result of calculations in the quasiclassical approximation (10) with the parameters (a) $R_N = 5.2$ fm, $a_0 = 1.0$; (b) $R_N = 4.4$ fm, $a_0 = 0.8$; and (c) $R_N = 4.4$ fm, $a_0 = 0.7$. Curves *3* in panels b and c mark the cross-section $\frac{d\sigma}{d\Omega} = \frac{1}{4}R_N^2$ at $U_0 \to \infty$ and the deuteron scattering angles $\theta_{\text{c.m.}} > 70°$, $R_N = 2$ fm

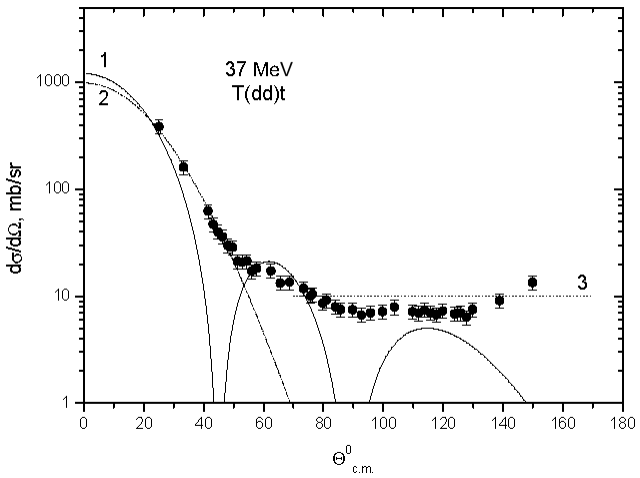

Fig. 5. Analysis of the elastic dt scattering in the models of black nuclei and nuclei with smeared boundaries: experiment, E_d = 37.0 MeV (points); calculation by formula (11) for black nuclei with $R_N = 4.4$ fm (curve *1*); calculation by formula (12) for nuclei with smeared boundaries and the parameters $B^2 = 0.12$ fm^{-2} and $a_{dt} = 2.1$ (curve *2*); the cross-section $\frac{d\sigma}{d\Omega} = \frac{1}{4}R_N^2$ at $U_0 \to \infty$ and the deuteron scattering angles $\theta_{\text{c.m.}} > 70°$, $R_N = 2$ fm (straight line *3*)

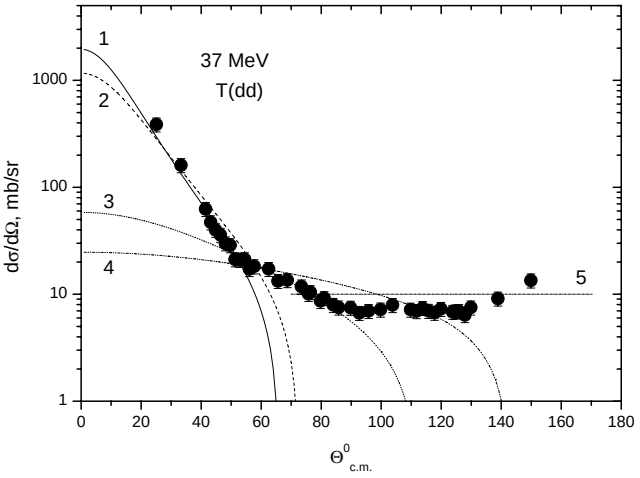

Fig. 6. Analysis of the elastic T(dd) scattering in the classical approximation with a finite U_0. Points are experimental data at E_d = 37.0 MeV. Curves *1* to *4* are the results of calculations by formula (13) with the parameters (*1*) R_N = 4.5 fm, U_0 = 9.35 MeV; (*2*) R_N = 4.2 fm, U_0 = 12.0 MeV; (*3*) R_N = 2.2 fm, U_0 = 50 MeV; and (*4*) R_N = 2.2 fm, U_0 = 200 MeV. Curve *5* marks the cross-section $\frac{d\sigma}{d\Omega} = \frac{1}{4}R_N^2$ at $U_0 \to \infty$ and the deuteron scattering angles $\theta_{\text{c.m.}} > 70°$, $R_N = 2$ fm

condition $kR_N \gg 1$, which provides the applicability of formula (10), is at the limit of its validity range, we observe a considerable interference between the diffraction and classical amplitudes (see curves *2* in Figs. 4,*a* and *b* calculated for the diffraction and classical cross-sections, respectively). This circumstance leads to the appearance of minima near $\theta_{\text{c.m.}} = 45$ and 85°, as well as adjacent broad diffraction maxima in the intervals $45° \le \theta_{\text{c.m.}} \le 85°$ and $85° \le \theta_{\text{c.m.}} \le 130°$ at an energy of 37 MeV. Since the interference in the cross-section for amplitude (10) is substantial at the energy concerned (the product kR_N is not large), it can be one of the reasons why only the qualitative description of the cross-section is possible, which is observed at the angles $\theta_{\text{c.m.}} > 60°$. Nevertheless, the θ-dependence is reproduced, in general, correctly at a qualitative level, if one makes allowance for a reduction of the effective interaction radius R_N at large angles and takes into account that the cross-section decreases, if the semitransparency of colliding nuclei is taken into consideration, as well as the errors of the momentum approximation. At large scattering angles, when the scattered deuteron flies backwards in the c.m.s. and the transferred momentum is large, the nuclei penetrate more deeply into each other, and the effective radius of interaction R_N diminishes together with the cross-section magnitude. Therefore, the approximation of impermeable nuclei is too rough in this case, as it was in work [16].

The reduction of the interaction radius R_N with increase in the scattering angle, when the momentum and energy transfers between nuclei get larger, agrees with the fact marked long ago [21–23] that R_N diminishes, when the relative energy of colliding nuclei grows. This phenomenon was confirmed (and explained) by calculations in the framework of the nuclear optical model.

If the energy of bombarding deuterons E_d decreases down to 29.15 MeV – and especially to 14.4 and 8.3 MeV – in the laboratory system [3,7], the mentioned theoretical maxima at angles $40° \le \theta \le 130°$, which arise "prematurely" according to formula (10) at $E_d = 37$ and 39.9 MeV, manifest themselves more soundly in experiment as well, in the form of a single diffraction maximum in the angular interval $70° \le \theta \le 130°$ at the energy E_d = 14.4 MeV (see Figs. 3 and 4,*a*). The cross-section values within this maximum interval are almost an order of magnitude smaller than those at small angles θ. It can be seen rather distinctly from Fig. 4,*a* for E_d = 14.4 MeV (the notations and the meaning of the curves are the same as in Figs. 4, *b* and *c*). The emergence of this observable maximum

can be explained at a qualitative level: it is associated with the appearance of the second calculated diffraction maximum, with the manifestation of a structure of colliding nuclei (i.e. the nuclei are not point-like). In particular, it is related with the formation of a singlet deuteron, its quasistationary state at scattering [3, 21], and the quantum-mechanical phenomena, namely, the interference between the quantum and classical amplitudes of scattering, when the contribution of the interference of diffraction and isotropic classical scatterings [16] at energies E_d of about $10 - 20$ MeV becomes much more weighty than at $E_d = 37.0$ and 39.9 MeV, i.e. when the product kR_N is only slightly larger than unity. The manifestation of a nuclear structure is also associated with the increase of cross-sections that is observed at large angles $\theta_{\text{c.m.}} \geq 130°$, when the deuteron obtains a considerable momentum, penetrates more deeply into the triton, and flies away almost in the opposite direction.

4.2. Models of black nuclei and nuclei with smeared boundary

The curves in Fig. 5, which were calculated in various approximations for $E_d = 37.0$ MeV, qualitatively confirm the aforesaid. Curve *1* ($R_N = 4.4$ fm) demonstrates the dependence of the cross-section $\frac{d\sigma}{d\Omega}$ on the scattering angle $\theta_{\text{c.m.}}$ in the simplest model of colliding nuclei considered as black balls with sharp boundaries. In this case, the expression for the corresponding amplitude duplicates the first term on the right-hand side of Eq. (10):

$$\frac{d\sigma}{d\Omega} = \frac{R_N^2}{4\sin^2\frac{\theta}{2}} J_1^2\left(2kR_N \sin\frac{\theta}{2}\right), \quad R_N = 4.4\,\text{fm}. \tag{11}$$

The secondary diffraction maxima in dependence (11) appear due to the assumption that colliding nuclei have sharp boundaries. The tops of those maxima, as is seen from Fig. 5, "prop up" the experimental points at the angles $\theta \geq 60°$. The first and second secondary maxima at $\theta \geq 60°$ are evidently the main reason for the maximum at $70° \leq \theta \leq 130°$ (in Fig. 4,*a* for $E_d = 14.4$ MeV) to appear.

For the sake of comparison, the cross-section for a deuteron and a triton with smeared boundaries, which penetrate into each other, is given in Fig. 5 (curve *2*). The cross-section is qualitatively described by a general profile function of the Gaussian-like type $\omega_{dt}(R) = a_{dt}e^{-B^2R^2}$, where R is the distance between nuclear centers:

$$\frac{d\sigma}{d\Omega} = \frac{a_{dt}^2 k^2}{4B^4} \exp\left(-\frac{2k^2\sin^2\frac{\theta}{2}}{B^2}\right),$$

$$a_{dt} = 2.1,\ B^2 = 0.12 \quad \text{fm}^{-2}. \tag{12}$$

The secondary maxima in cross-section (12), in contrast to formula (11), do not appear; i.e. expression (12) can satisfactorily describe only the main maximum in the cross-section at small angles $\theta < 60°$. (This result is a certain justification for the application of the momentum approximation with profile functions (1) and the corresponding cross-section (9).) Hence, the real cross-section can be better described at large angles θ by a dependence that is intermediate between those two cases, (11) and (12). For instance, if the profile function is selected in the form of the Fermi dependence, the cross-section cannot be obtained in the explicit form (in this case, amplitude (3) for such ω_{ij} remains an 11-multiple integral).

4.3. Classical approximation with finite U_0

Since our consideration of the dt scattering is quasiclassical, there appears a certain interest to make comparison of our experimental and theoretical results for the cross-sections given above with the limiting ($\lambda\!\!\!^{-}/R_N \to 0$) classical scattering cross-section for the finite (in contrast to work [16]) potential energy U_0 (in the form of a rectangular well) of interaction between nuclei considered as balls [25]:

$$\frac{d\sigma}{d\Omega} = \frac{R_N^2\eta^2}{4\cos\frac{\theta}{2}} \frac{\left(\eta\cos\frac{\theta}{2} - 1\right)\left(\eta - \cos\frac{\theta}{2}\right)}{\left(1 + \eta^2 - 2\eta\cos\frac{\theta}{2}\right)^2},$$

$$\eta = \sqrt{1 + \frac{5U_0}{3E_d}},\ 0 \leq \theta \leq \theta_{\max},\quad \theta_{\max} = 2\arccos\frac{1}{\eta}. \tag{13}$$

Figure 6 illustrates the dependence of this cross-section on θ (at $E_d = 37.0$ MeV) for various values of the parameters R_N and U_0. The ratio $\lambda\!\!\!^{-}/R_N \approx 0.1 \div 0.2$ in this case. If $U_0 \to \infty$, cross-section (13) becomes constant $\left(\frac{d\sigma}{d\Omega} = \frac{1}{4}R_N^2\right)$ and coincides with the corresponding classical (isotropic) cross-section obtained in work [16].

One can see that classical cross-section (13) cannot adequately describe the observable angular dependence simultaneously within the whole angular interval $25° < \theta < 150°$, irrespective of the selected U_0-value, without

taking into account quantum-mechanical effects and the real structure of colliding nuclei. Nevertheless, in some θ-intervals, the qualitative description can be obtained. It is especially true for a nuclear potential well with the depth $U_0 = 50$ MeV close to the real value. In this case, a quite good quantitative agreement with the experiment is observed at $E_d = 37.0$ MeV. One can see that the classical model qualitatively explains the cross-section reduction at a decrease of the potential well depth U_0, which is observed for large angles $\theta > 70°$. At the same time, the classical cross-section cannot, of course, explain such a quantum-mechanical phenomenon as the emergence of a diffraction maximum in the range of small angles $\theta < 70°$ at $U_0 \geq 50$ MeV, which is observed in experiment.

Figures 4(b and c), 5, and 6 demonstrate that, at the energies $E_d = 37 \div 40$ MeV, the cross-sections that are observed in the broad region of the smooth minimum at $70° \leq \theta \leq 140°$ hardly reach a magnitude of 10 mb/sr. Since the angles are rather large in this interval, then, according to work [16], one can approximately adopt the simple relation $\frac{d\sigma}{d\Omega} = \frac{1}{4}R_N^2$ for this region; whence, $R_N \approx 2$ fm for $\frac{d\sigma}{d\Omega} \approx 10$ mb/sr. Straight lines *3* in Figs. 4(b and c) and 5 and straight line *5* in Fig. 6 give the corresponding qualitative illustration of the cross-section behavior at the energies $E_d \approx 30 \div 40$ MeV and large deuteron scattering angles $\theta > 70°$, when $R_N = 2$ fm.

4.4. Analysis of energy spectra

The distributions of scattered deuterons, $\frac{d\sigma}{d\Omega_d dE'_d}$, over their energy E'_d and recoil tritons, $\frac{d\sigma}{d\Omega_t dE_t}$, over their recoil energy E_t in the laboratory reference frame, where tritons do not move before the collision, at the deuteron scattering angles $\theta_d = 15$ and 38° (Fig. 2,a), and the triton exit angles $\theta_t = 15$ and 38° (Fig. 2,b)—those distributions were measured in our experiment—were described theoretically at $E_d = 37$ MeV making use of the formulas of the microscopic diffraction model given above [20]. As is seen from those figures, the positions, widths, and heights of maxima in the corresponding observed differential cross-sections are described well in the indicated approximation by the following expressions obtained by us for the cross-sections:

$$\frac{d\sigma}{d\Omega_d dE'_d} = \frac{9M\sqrt{E_d E'_d}}{5\pi^2}\times$$

$$\times\,|A(\chi)|^2\,\delta(5E'_d - E_d - 4\sqrt{E_d E'_d}\cos\theta_d), \qquad (14)$$

$$\frac{d\sigma}{d\Omega_t dE'_t} = \frac{3^{3/2}M\sqrt{E_d E'_t}}{5\sqrt{2}\pi^2}\times$$

$$\times\,|A(\chi)|^2\,\delta(2\sqrt{6E_d E_t}\cos\theta_t - 5E_t), \qquad (15)$$

where the amplitude $A(\chi)$ was taken in the same form as in formulas (3), (4), and (9); and $d\Omega_d$ and $d\Omega_t$ are the elements of solid angles in the l.s., where the momenta of a scattered deuteron and a recoil triton, respectively, fall within. The quantity χ in $A(\chi)$ was expressed in terms of kinematic variables in the l.s. In particular, $\chi = [4M(E_d + E'_d - 2\sqrt{E_d E'_d}\cos\theta_d)]^{1/2}$ was substituted into Eq. (14) and $\chi = \sqrt{6ME_t} = \frac{12}{5}\sqrt{ME_d}\cos\theta_d$ into Eq. (15). Here, E'_d and θ_d are the final energy and the scattering angle of a deuteron in the l.s., and E_t and θ_t are their counterparts for recoil tritons. We used the relations between the scattering angles and the energies of nuclei in the c.m.s. and l.s. before and after collisions, which were given in works [19, 25, 26]. We also took advantage of the fact that the cross-section differential $d\sigma$ is invariant, if changing over from the c.m.s. to the l.s. When calculating the cross-sections by formulas (14) and (15), the corresponding delta-functions $\delta(E)$ were replaced by a finite function of the Breit–Wigner type, $\delta_\Gamma(E)$, whose acute peaks were characterized by a finite width Γ:

$$\delta_\Gamma(E) = \frac{\Gamma}{2\pi}\frac{1}{E^2 + \frac{1}{4}\Gamma^2}, \;\; \lim\delta_\Gamma(E) = \delta(E), \;\; \Gamma \to 0. \;\; (16)$$

The application of the Gaussian dependence instead of expression (16) for $\delta_\Gamma(E)$ brings about similar results.

The results of energy distribution calculations, which were fulfilled in the framework of the microscopic diffraction model, agree satisfactorily with experimental data at the values $\Gamma = 0.68 \div 0.69$ MeV ($\theta_{\text{l.s.}} = 15 \div 38°$) for deuterons and $\Gamma = 0.92 \div 1.04$ MeV ($\theta_{\text{l.s.}} = 15 \div 38°$) for recoil tritons. An appreciable, although rather small, value of the cross-section $\frac{d\sigma}{d\Omega_t dE_t}$ at $\theta_t = 15°$ (Fig. 2,b) for practically all possible recoil triton energies $E'_t > 15$ MeV and not only near the maximum at $E_t \approx 32$ MeV draws attention. This circumstance is associated with the fact that the absolute value of the recoil triton momentum, which is equal to the transferred momentum modulus $|\mathbf{k}_d - \mathbf{k'}_d|$, where $\mathbf{k'}_d$ is the momentum of the scattered deuteron, is large, as well as the energy E_t, at small angles θ_t and the energies $E_t > 15$ MeV. Therefore, the internal degrees of freedom of the colliding triton and deuteron can be excited with

an appreciable probability. Both particles transit for a short time into virtual intermediate quasistationary states, which were mentioned above. Later on, they can either return back with a certain probability into their initial bound states (the corresponding process of elastic scattering is observed in our experiment) or can decay to create new particles, which we did not register experimentally.

5. Conclusions

1. The differential cross-sections for elastic scattering of deuterons with the energy $E_d = 37$ MeV by tritons in the range of scattering angles $25° \leq \theta_{\text{c.m.}} \leq 150°$ have been obtained.
2. The elastic scattering of deuterons with energies of 14.4 [7], 37.0 (our data), and 39.9 MeV [11] by tritons (helions) has been analyzed in the framework of the microscopic diffraction nuclear model and making allowance for NN interactions. The observed angular distributions of scattered deuterons in the range of the main maximum ($\theta_{\text{c.m.}} \leq 60°$) are described rather well at energies of 14.4, 37, and 39.9 MeV.
3. The angular distribution cannot be described adequately well in the whole region $25° \leq \theta_{\text{c.m.}} \leq 150°$ simultaneously by phenomenological quasiclassical approximations without a rigorous account of quantum-mechanical diffraction effects and the real structure of colliding nuclei. A qualitative description was obtained in the angular interval $60° < \theta_{\text{c.m.}} < 150°$. A satisfactory quantitative agreement with experiment at $E_d = 37.0$ MeV was obtained in the angular interval $50° < \theta < 90°$ for the depth of the nuclear potential well $U_0 = 50$ MeV, which is close to the actual value.
4. An explanation has been proposed for the appearance of a broad secondary maximum in the cross-section dependence on the deuteron scattering angle in the interval $70° \leq \theta \leq 130°$ and at the energies of incident deuterons 6.0 MeV $\leq E_d <$ 29 MeV. The maximum was shown to arise owing to the interference between the quantum and classical isotropic amplitudes of scattering and as the manifestation of a structure of colliding nuclei.
5. The analysis of the energy spectra of deuterons and recoil tritons in the dt reaction at an energy of 37 MeV has been carried out. The results of energy distribution calculations in the framework of the microscopic diffraction nuclear model agree well with experimental data at $\Gamma = 0.68 \div 0.69$ MeV ($\theta_{\text{l.s.}} = 15 \div 38°$) for deuterons and $\Gamma = 0.92 \div 1.07$ MeV ($\theta_{\text{l.s.}} = 15 \div 38°$) for recoil tritons.

1. O.O. Belyuskina, S.V. Berdnichenko, V.I. Grantsev *et al.*, Yad. Fiz. Energ. N 3, 54 (2007).
2. M. Ivanovich, P.G. Young, and G.G. Ohlsen, Nucl. Phys. A **110**, 441 (1968).
3. V.M. Lebedev, V.G. Neudachin, and B.G. Struzhko, Yad. Fiz. **65**, 1 (2002).
4. V.I. Konfederatenko, B.G. Struzhko, and O.M. Povoroznyk, Ukr. Fiz. Zh. **39**, 393 (1994).
5. G. Calvi, M. Lattuada, F. Riggi *et al.*, Phys. Rev. C **44**, 325 (1991).
6. V.O. Aleshin, O.O. Belyuskina, S.V. Berdnichenko *et al.*, in *Proceedings of the International Conference "Current Problems in Nuclear Physics and Atomic Energy"* (Kyiv, 2007), Pt. 1, p. 27 (in Ukrainian).
7. J.E. Brolley, jr., T.M. Putnam, L. Rosen, and L. Stewart, Phys. Rev. **117**, 1307 (1960).
8. V.K. Tartakovskii, A.V. Fursaev, and B.I. Sidorenko, Yad. Fiz. **68**, 35 (2005).
9. V.I. Grantsev, V.O. Grashylin, Yu.O. Dei *et al.*, Zbirn. Nauk. Prats Inst. Yad. Dosl. N 1, 108 (2004).
10. T.R. King and S. Rotman, Nucl. Phys. A **183**, 657 (1972).
11. R. Roy, F. Seiler, H.E. Conzett, and F.N. Rad, Phys. Rev. C **24**, 2421 (1981).
12. O.I. Akhiezer and O.G. Sitenko, Ukr. Fiz. Zh. **3**, 16 (1958).
13. R. Glauber, Usp. Fiz. Nauk **103**, 641 (1971).
14. A.A. Arkhipov, Fiz. Elem. Chastits At. Yadra **38**, 1451 (2007).
15. V.I. Grantsev, V.V. Davydovskyy, K.K. Kisurin *et al.*, Probl. At. Sci. Tech. N 5, 13 (2007).
16. V.M. Galitskii, B.M. Karnakov, and V.I. Kogan, *Problems in Quantum Mechanics* (Nauka, Moscow, 1981) (in Russian).
17. O.G. Sitenko and V.K. Tartakovskii, Ukr. Fiz. Zh. **6**, 12 (1961).
18. V.K. Tartakovskii and V.I. Koval'chuk, Zh. Fiz. Dosl. **10**, 29 (2006).
19. L.D. Landau and E.M. Lifshitz, *Quantum Mechanics. Non-Relativistic Theory* (Pergamon, New York, 1965).
20. V.K. Tartakovskii, Izv. Vyssh. Ucheb. Zaved. SSSR Fiz. N 9, 3 (1980).
21. K. Suth, Nucl. Phys. A **138**, 61 (1969).
22. Yu.A. Berezhnoi and N.A. Shlyakhov, Ukr. Fiz. Zh. **21**, 192 (1976).
23. M.V. Evlanov, A.M. Sokolov, and V.K. Tartakovskii, Yad. Fiz. **66**, 278 (2003).
24. K.O. Terenetskii, Yad. Fiz. **37**, 1177 (1983).
25. L.D. Landau and E.M. Lifshitz, *Mechanics* (Butterworth Heinemann, Oxford, 2001).
26. A.S. Davydov, *Theory of Atomic Nucleus* (Nauka, Moscow, 1958) (in Russian).

Received 07.08.08.
Translated from Ukrainian by O.I. Voitenko

ПРУЖНЕ РОЗСІЯННЯ ДЕЙТРОНІВ НА ТРИТОНАХ

О.О. Белюскіна, В.І. Гранцев, В.В. Давидовський, К.К. Кісурін, С.Є. Омельчук, Г.П. Палкін, Ю.С. Рознюк, Б.А. Руденко, Л.С. Салтиков, В.С. Семенов, Л.І. Слюсаренко, Б.Г. Стружко, В.К. Тартаковський, В.А Шитюк

Р е з ю м е

Експериментально досліджено диференціальні перерізи пружного розсіяння дейтронів з енергією $E_d = 37,0$ МеВ на тритонах у діапазоні кутів розсіяння $25^\circ \leq \theta_{\text{ц.м.}} \leq 150^\circ$. Проведено аналіз кутових розподілів пружного розсіяння дейтронів на тритонах (геліонах) при енергіях 14–40 МеВ за мікроскопічною дифракційною моделлю з урахуванням NN-взаємодії, що дозволило задовільно описати цією моделлю кутові розподіли дейтронів у діапазоні основного максимуму ($\theta_{\text{ц.м.}} \leq 60^\circ$) при $E_d = 14,4$; $37,0$ і $39,9$ МеВ. Запропоновано пояснення природи появи широкого вторинного максимуму при низьких енергіях дейтронів, проведено розрахунки та показано, що він з'являється завдяки інтерференції квантової та класичної ізотропної амплітуд розсіяння і прояву структури взаємодіючих ядер. Характерні особливості кутової залежності dt-перерізів в області кутів розсіяння $60^\circ \leq \theta_{\text{ц.м.}} \leq 130^\circ$, що виникають при збільшенні енергії від 6 до 40 МеВ, вдалося пояснити лише якісно, використовуючи феноменологічне квазікласичне наближення. Проведено аналіз енергетичних спектрів дейтронів і тритонів віддачі з реакції T(dd)T при $E_d = 37,0$ МеВ.